

Detection and Classification of Disturbances in DG Based Power System using Time-Frequency-Scale Transform

Anshuman Bhuyan
Department of EE
Gandhi Institute for Education &
Technology
Bhubaneswar, India
bhuyananshuman@gmail.com

Basanta K. Panigrahi
Department of EE, ITER
Siksha 'O' Anusandhan
Bhubaneswar, India
basanta1983@gmail.com

Jyoti Shukla
Department of EE
SKIT M & G, Jaipur
Jaipur, India
j.shukla111@gmail.com

Kumaresh Pal
Department of Electrical Vehicle
Tata Steel Foundation
Jamshedpur, India
kumaresh.pal@rediffmail.com

Subhendu Pati
Department of EE, ITER
Siksha 'O' Anusandhan
Bhubaneswar, India
subhendupati90@gmail.com

Abstract— Penetration of solar energy into conventional power grid generates an issue of operation and control, creating a challenge to identify fault disturbances in electrical power system. This paper discusses a novel method for tracking fault disruptions under various working circumstances. Various fault disturbances such as LL, LLL, LG, LLG, & LLLG are considered for the present study. Statistical features are determined using wavelet and Hyperbolic S-transform to formulate a feature dataset to be processed through the classification techniques. The feature data set will greatly reduce the size thereby reducing computational burden on the identification techniques. The efficiency of detection and classification is improved as a result of the reduced complexity in recognizing the disturbances. Decision trees (DT) & support vector machines (SVM) are two examples of pattern recognition systems used to categorize fault disturbances. These studies show that when HS-transform is combined with DT, it provides the best attainable accuracy, which demonstrates its reliability under a wide range of operational conditions, including load variation, solar insolation, harmonics, & noise in the scheme's parameters.

Keywords— Detection, Classification, decision tree, fault disturbance, HS-transform, support vector machines, distributed generation (DG).

I. INTRODUCTION

To meet the rising demand for power, renewable energy in the form of distributed generation (DG) is quickly becoming a prime contribution due to its merits as green energy with relatively few atmospheric pollutions [1]. Solar and wind power are the most flexible renewable options. Although they have a great deal of untapped potential, their integration into the existing power grid presents a number of operational & design challenges for power systems. Whether the faults are symmetrical or asymmetrical, they can have a significant impact on the system if they disrupt its stability. Once again,

when the photovoltaic system that runs on solar power is wired into the grid via interface converters [2]. The maintenance of a reliable power supply to the consumers is a crucial component of power system architecture. However, this situation is hampered by the various fault disruptions brought about in the power system by natural disasters, human error, physical mishaps, lightning, and other operational problems. These will result in fault circumstances like LG, LL, LLG, LLL, and LLLG, which could endanger the stability and dependability of the power supply directly or indirectly [3]. Numerous studies for identifying and tracking fault disturbances were published in the literature. The most extensively used approaches for investigating disturbances are Fourier Transform (FT) and Fast Fourier Transform (FFT). In order to achieve the goals of fault analysis, many techniques like S-transform, wavelet transform (WT) & short-time Fourier Transform (STFT) were developed [4].

Additionally, many artificial intelligence techniques, including support vector machines (SVM), artificial neural networks (ANN), fuzzy logic (FL), and Decision Tree (DT), are utilized to categorize the fault disturbances. Popular applications of ANN include fault detection, localization, and classification [5]. The wavelet transform and ANN were proposed together to identify the fault disturbances. Incorrect phase/section identification in the power system was handled using fuzzy logic [6]. Fuzzy logic and neural networks, in the form of ANFIS, are applied correctly and successfully to achieve the same goals of safeguarding the electrical grid and its components. A further candidate for fault categorization is support vector machines (SVM) [7]. These studies, however, present a wavelet/HS-transform, SVM, & DT hybrid methodology to a fault detection and classification. This is because some of the aforementioned techniques perform worse when there is a higher penetration on renewable energy

sources, anomalous operating conditions in power systems owing to the presence of noise, and unreliable system inputs such as solar insolation in solar PV systems. It has been demonstrated that the HS-transform performs better in noisy situations when paired with DT and SVM for appropriately identifying the disturbances [8].

The paper is structured as shown below. Section II provides a details of the PV-based system configuration. The proposed approaches are described in Section III, while Section IV is devoted to the simulation results and related discussion. Last but not least, Section V summarizes the research's conclusions.

II. SYSTEM CONFIGURATION OF SOLAR ENERGY-BASED POWER SYSTEM

Solar energy is a crucial renewable source of power that is employed in the current studies and is integrated with the traditional electrical system. It has numerous uses in society. The next subsections provide modeling & explanations of such a system.

A. System Configuration

A solar PV system is shown in Fig. 1 that is incorporated with a battery energy storage system and connected to the regular power grid. A bi-directional converter during times of strong solar insolation stores the excess energy in the battery. For the purpose of studying disturbances, the system in Fig. 1 is adopted. As depicted in Fig. 1, which is a straightforward block diagram/configuration of a solar energy-based system with several components. While Fig. 2 illustrate the precise interface topology of the power system under consideration.

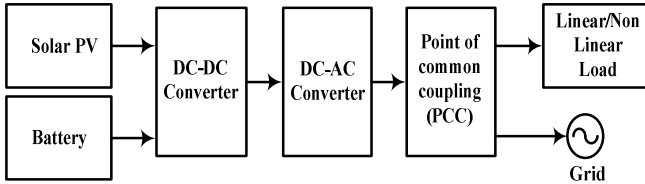


Fig. 1. block diagram of a solar-based system

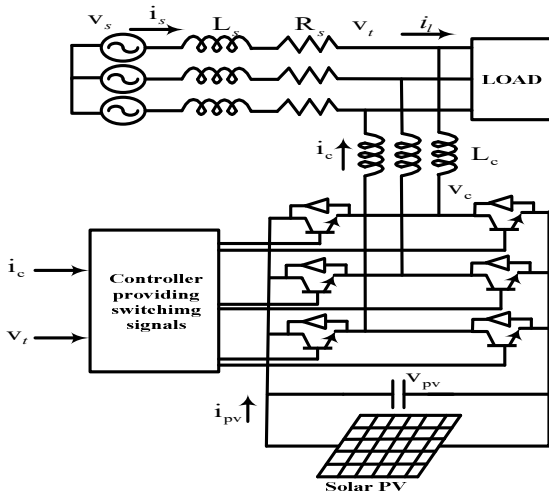


Fig.2 Interfacing circuit of solar based power system

B. PV cell/array modeling

The photovoltaic (PV) cell, which turns sunlight into electricity, is structurally comparable to a p-n junction. An internal series resistance R_s and a shunt resistance R_{sh} , along with a photo-current source I_{ph} and a non-linear diode, constitute the equivalent circuit representation of a solar cell. The mathematical equation representing a solar cell is presented by:

$$I = I_{ph} - I_s \left(e^{\frac{q}{AKT}(V+IR_s)} - 1 \right) - \frac{1}{R_{sh}}(V + IR_s) \quad (1)$$

I_{ph} represents the photo-current, I_s , the diode's saturation current, A is the diode's ideality factor, q the electron charge, k Boltzmann's constant and S the solar intensity in watts per square meter. Temperature and solar intensity are used to get a formula for the photo-current is presented by:

$$I_{ph} = \left(\frac{S}{S_{ref}} \right) \left[I_{ph,ref} + C_T(T - T_{ref}) \right] \quad (2)$$

Where S_{ref} , is the reference value for solar intensity, T_{ref} is the reference value for cell temperature, and $I_{ph,ref}$ is the reference value for photocurrent, temperature coefficient is C_T . Under conventional test conditions & the semiconductor material's band energy gap, the diode saturation current is denoted by the symbols $I_{s,ref}$ and E_g , respectively. Cells incorporated in parallel & series are combined to form a PV module. The voltage current characteristic equation of the equivalent model is:

$$I = N_p I_{ph} - N_p I_s \left(e^{\frac{q}{AKT} \left(\frac{V + IR_s}{N_s + N_p} \right)} - 1 \right) - \frac{N_p}{R_{sh}} \left(\frac{V + IR_s}{N_s + N_p} \right) \quad (3)$$

N_s is for the total number of cells connected in a series, and N_p stands for the total number of cells connected in parallel.

III. PROPOSED METHODOLOGIES

The descriptions of various detection and classification such as HS-transform ,DT and SVM are described below..

A. HS-transform

A time-frequency multi-resolution analysis called S-transform (ST), which is a modified WT with phasor correction, is created using WT and STFT. It makes use of a Gaussian variable window, where the relationship between width and frequency is inverse. But occasionally the S-transform is unable to identify disturbances, even when there is noise present. Therefore, the HS-transform using a pseudo-hyperbolic Gaussian window provides superior temporal & frequency resolutions across the entire frequency spectrum, from the lowest to highest. An increase in the window's low-frequency asymmetry results in a wider frequency domain. [9].

The equation for the hyperbolic window is:

$$W_{hb} = \frac{2f_s}{\sqrt{2\pi(\alpha_{hb} + \beta_{hb})}} \exp\left\{-\frac{f_s^2 X^2}{2}\right\} \quad (4)$$

Where

$$X = \frac{(\alpha_{hb} + \beta_{hb})}{2\alpha_{hb}\beta_{hb}}(\tau - t - \xi) + \frac{(\alpha_{hb} - \beta_{hb})}{2\alpha_{hb}\beta_{hb}}\sqrt{(\tau - t - \xi)^2 + \lambda_{hb}^2}$$

$$0 < \alpha_{hb} < \beta_{hb} \text{ and } \xi = \frac{\sqrt{(\beta_{hb} - \alpha_{hb})^2 \lambda_{hb}^2}}{4\alpha_{hb}\beta_{hb}} \quad (5)$$

The discrete version of the HS-transform is calculated, and $G(m_F, n_F)$ stands for the Fourier transform of the hyperbolic window.

$$G(m_F, n_F) = \frac{2f_s}{\sqrt{2\pi(\alpha_{hb} + \beta_{hb})}} \exp\left\{-\frac{f_s^2 X_D^2}{2}\right\} \quad (6)$$

Where:

$$X_D = \frac{(\alpha_{hb} + \beta_{hb})}{2\alpha_{hb}\beta_{hb}}t + \frac{(\alpha_{hb} - \beta_{hb})}{2\alpha_{hb}\beta_{hb}}\sqrt{t^2 + \lambda_{hb}^2} \quad (7)$$

$H[m_F, n_F]$ is the frequency shifted Fourier transform $H[m_F]$ and given by:

$$H[m_F] = \frac{1}{N} \sum_{m_F=0}^{N-1} h(k) \exp(-i2\pi n_F k) \quad (8)$$

$$S[n_F, j] = \sum_{m_F=0}^{N-1} H(m_F + n_F) G(m_F, n_F) \exp(-i2\pi m_F j) \quad (9)$$

B. Decision tree (DT)

Comparisons between data sets can be used to categorize the information. Decision trees can be used effectively for data classification. Repeatedly, these characteristics are broken down into new cases until the right conclusion & classification are reached[10]. Following is a mathematical representation of a Decision Tree:

$$\bar{X} = \{X_1, X_2, \dots, X_m\}^T \quad (10)$$

$$X_i = \{x_1, x_2, \dots, x_{ij}, \dots, x_{in}\} \quad (11)$$

$$S = \{S_1, S_2, \dots, S_i, \dots, S_m\} \quad (12)$$

Where S is the m-dimensional vector of the variable predicted from, X_i is the i^{th} component vector of n-dimension autonomous variables & $x_{i1}, x_{i2}, \dots, x_{ij}, \dots, x_{in}$ are autonomous variables of pattern vector X_i & T, where m is the number of observations and n is the number of independent variables. The following optimization problem is used to build a DT T_{k0} that is optimal in terms of size:

$$\hat{R}(T_{k0}) = \min_k \{\hat{R}(T_k)\}, \quad k = 1, 2, 3, \dots, K \quad (13)$$

$$\hat{R}(T) = \sum_{t \in \tilde{T}} \{r(t)p(t)\} \quad (14)$$

where $r(t)$ is the re-substitution estimation of error in misclassifying in node t and $p(t)$ is the possibility that any case drops into node t, T is a binary tree $\in \{T_1, T_2, T_3, \dots, T_k, t_1\}$, k is the index number of the tree, t is a tree node, with t_1 as the root node, and $\hat{R}(t)$ is the error level in misclassification of tree T_k . Sub-trees T^L and T^R are provided for left/right partition sets. T is constructed from features that divide a plane into equal parts. As shown in Fig.3, X might be binary partitioned into mutually exclusive left & right sets, for the bounds of 2-dimensional binary classification presented in Fig.4. Components of the lattice on the left have feature q values that are below the threshold, while those on the right have feature q values that are greater than the limit.

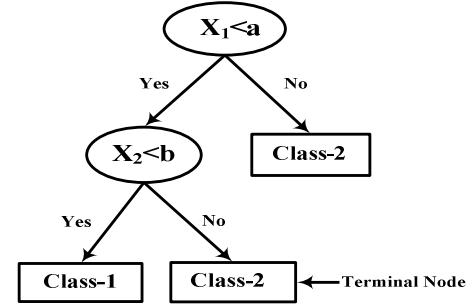


Fig. 3. Classification of DT based on threshold

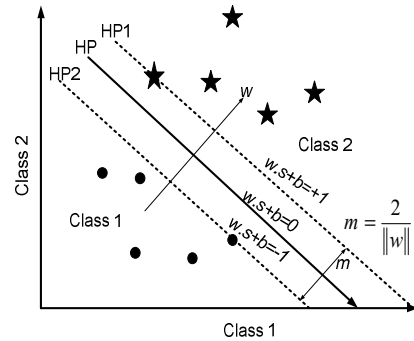


Fig. 4. hyper plane of support vector machine

C. Support vector machines (SVMs)

As a statistical learning technique for pattern categorization using a reduction of structural risk approach, support vector machines (SVMs) are a promising contender with superior generalization ability for high-dimensional data. Improved accuracy in fault categorization over both ANN & Bays classifiers has made SVM a popular choice for this task. For n-dimensional inputs $s_i (i = 1, 2, \dots, M)$, M is the number of samples that best fit into class1 or class2 with $o_i = 1$ for class1 and $o_i = -1$ for class2. $\|w\|^{-2}$ is given as the offset from the geometry [11]. The best hyperplane can be determined by solving the following optimization problem:

$$\frac{1}{2} \|w\|^{-2} + C \sum_{i=1}^M \xi_i \quad (15)$$

subject to:

$$o_i(w^T s + b) \geq 1 - \xi_i \quad \text{for } i = 1, 2, \dots, M \quad (16)$$

The unknown data sample s is categorized as:

$$s \in \begin{cases} \text{Class - 1, } f(s) \geq 0 \\ \text{Class - 2, otherwise} \end{cases} \quad (17)$$

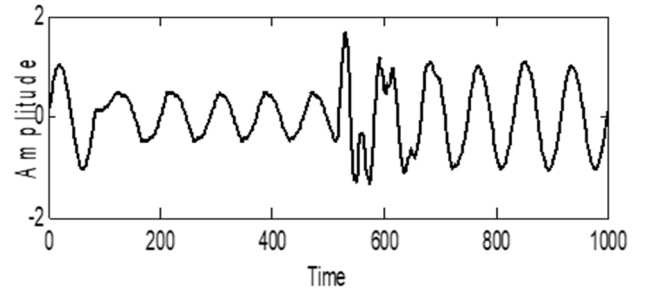
IV. RESULTS AND DISCUSSIONS

The results of MATLAB and Simulink simulations are discussed here. The entire simulated solar PV system, including the grid connection, is run through MATLAB. Whenever a grid failure is generated, the appropriate voltage signal is disabled at the PCC. Wavelet and HS-transforms are then applied to the data. Different statistical properties, such as dispersion and entropy, are computed from the converted signal. Next, six different characteristics and faults in various working scenarios are taken into account as data for a 500x6 information set. This data set is split in half, with one half utilized for training and the other for evaluation. This is how the various faults are classified. The various disturbances sampled from the system under investigation are listed in Table 1. At PCC, we assume that the sampling rate for the accumulated signal is 5 kHz. The HS-contour, the standard deviation, the mean, and the entropy of the magnitude and phase distributions are the inputs into the HST matrix, which is used to produce six statistical features.

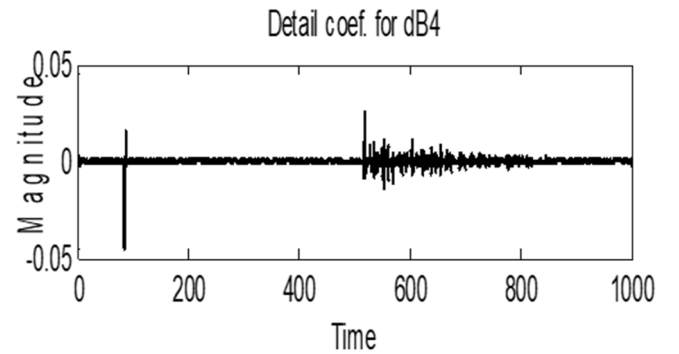
Table 1. Signal for study of fault disturbances

Signal class	Signal Description
C1	AG fault
C2	BG fault
C3	CG fault
C4	ABG fault
C5	BCG fault
C6	CAG fault
C7	ABC fault

The voltage signal for an AG fault as received at PCC is depicted in Fig. 5 (a). Fig. 5 (b) and Fig. (c) display the outcomes of this signal's transmission via WT and HST. Both the transform and the disruption instants in the voltage are clearly identified. Of course, HST has superior time-frequency resolution compared to WT. In addition, Fig. 6 depicts the result of adding 20 dB of noise to the voltage signal. As demonstrated in fig.6. (a), when traveling through WT and HST. In fig. 6. (b) and fig. 6. (c), it is determined that WT fails to recognize the signal because of noise, whereas in HST, the signal disruptions at the relevant times are beautifully caught and detected. This demonstrates how effectively HST performs in noisy conditions. Again, Fig. 7 (a) displays the retrieved voltage signal for an LLL fault. In Fig. 7 (b) and fig. (c), we can see the before-and-after outcomes of running the data through WT and HST, respectively. The detection power of HST has been found to be superior to that of WT. The outcomes are the same when using a noise level of 20 dB. In Fig. 8 (a) and fig.(b), we can see the categorization accuracy of SVM & DT for two different levels of noise. It is established that DT consistently outperforms SVM in terms of productivity. In addition to the border plot shown in Fig. 8 (c), which differentiates between three classes of fault disturbances (classes 1-3), a similar curve or contour may be provided in all other cases to do the same.



(a)



(b)

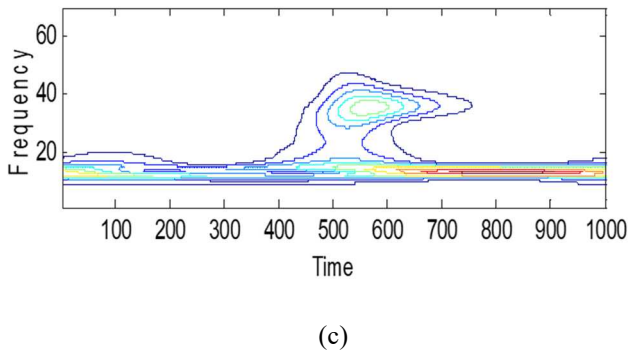


Figure 5. AG fault detection, (a) voltage signal for AG fault at PCC, (b) detection of fault by WT, (c) detection of fault by HST

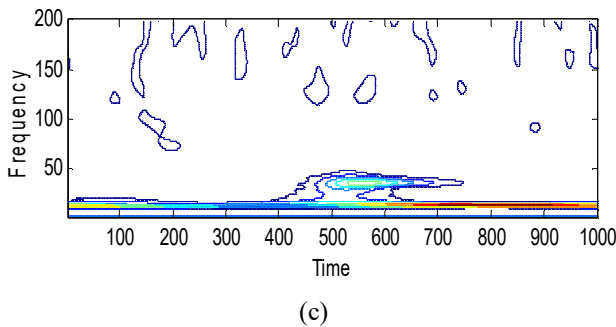
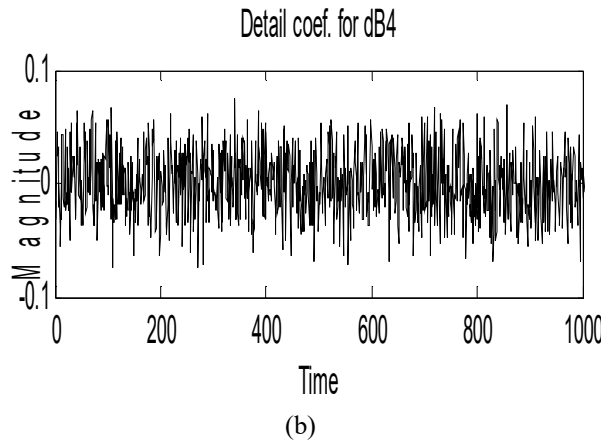
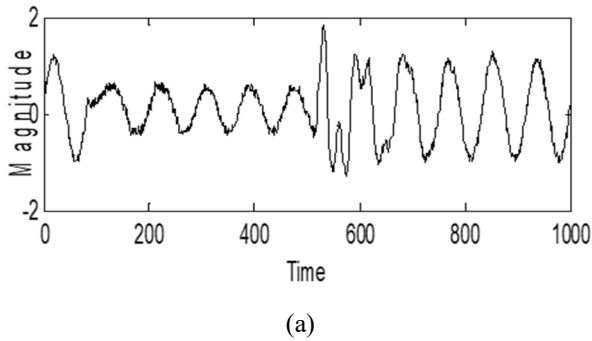


Fig. 6. AG fault detection with 20 dB noise, (a) voltage signal for AG fault at PCC with 20dB noise, (b) detection of fault by WT, (c) detection of fault by HST

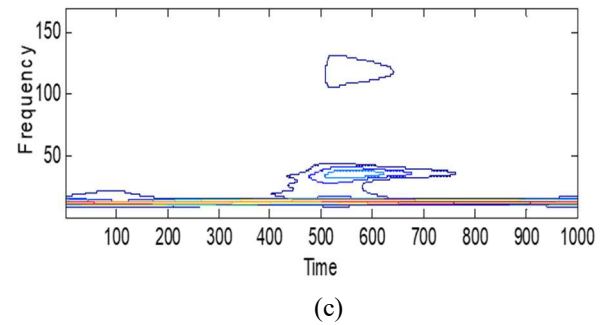
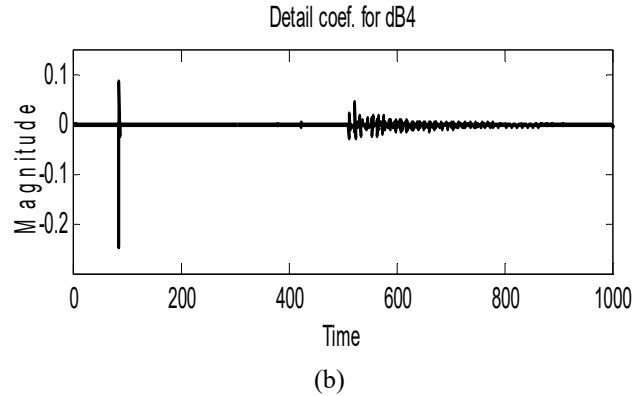
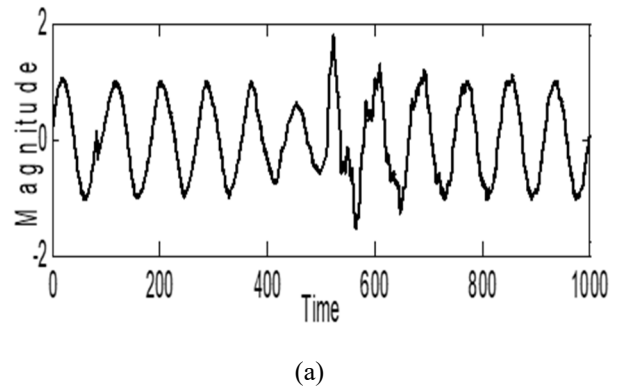
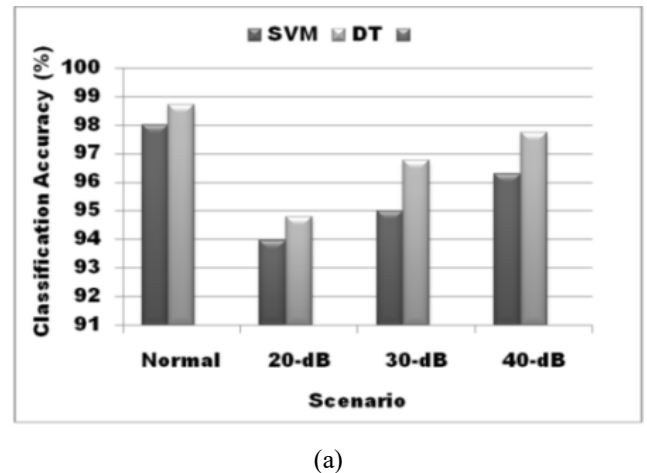
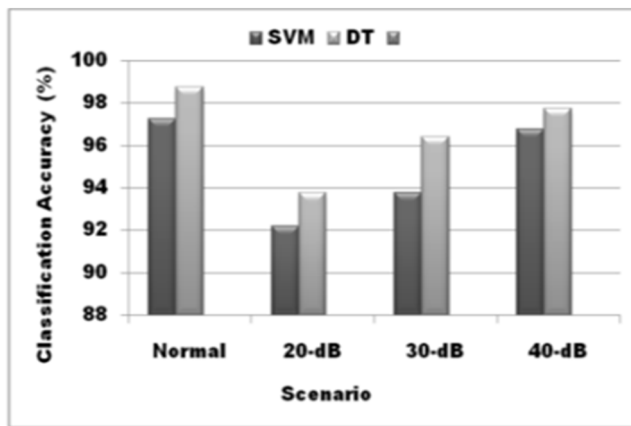
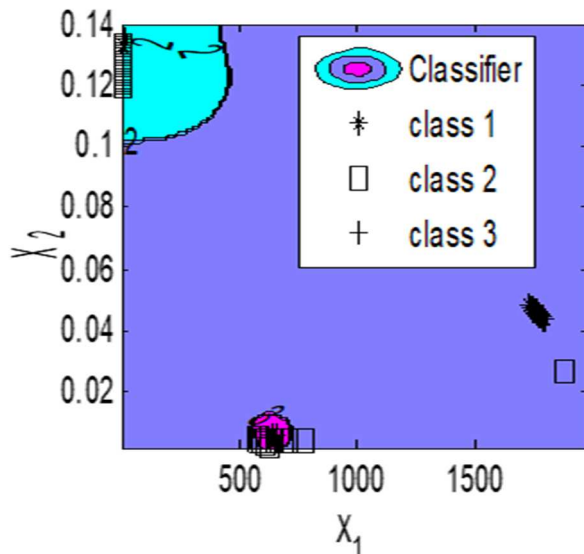


Fig. 7. LLL fault detection, (a) voltage signal for ABC fault at PCC, (b) detection of fault by WT, (c) detection of fault by HST





(b)



(c)

Fig. 8. classification of fault using SVM & DT, (a) for LL fault, (b) for LLG fault, (c) boundary plot to classify faults using SVM.

V. CONCLUSIONS

The analysis of various fault disturbances of a grid-connected PV-based power system has been described in the paper. The emergence of fault disturbances is caused not only by load shift but also by changes in environmental conditions like solar insolation. The fault disruptions were found using WT & HS-transform, and the classification was done using SVM and DT. The HS-transform was shown to be more precise in the detection of disturbances. Once more, it is determined that WT performance suffers when noise is added to the voltage signal. Despite the fact that HST was able to detect the signal's interference. The classification accuracy is significantly increased when the HS-transform is used with SVM/DT. A comparison of working conditions found that the DT's predicted classification precision outperformed the SVM's.

REFERENCES

- [1] Bhuyan, A., Panigrahi, B. K., & Pati, S. (2022). Fault Classification in a DG Connected Power System using Artificial Neural Network. *Indonesian Journal of Electrical Engineering and Informatics (IJEI)*, 10(2), 498-507.
- [2] Panigrahi, B. K., Bhuyan, A., Satapathy, A. K., Pattanayak, R., & Parija, B. (2020). Fault analysis of grid connected wind/PV distributed generation system. In *ICICCT 2019–System Reliability, Quality Control, Safety, Maintenance and Management: Applications to Electrical, Electronics and Computer Science and Engineering* (pp. 47-54). Springer Singapore.
- [3] Samantaray, S. R., Dash, P. K., & Panda, G. (2006). Fault classification and location using HS-transform and radial basis function neural network. *Electric Power Systems Research*, 76(9-10), 897-905.
- [4] Sarwagya, K., & Ranjan, S. (2020, January). Detection and Classification of Faults in Distribution System Using Signal Processing Techniques. In *2020 International Conference on Computer, Electrical & Communication Engineering (ICCECE)* (pp. 1-6). IEEE.
- [5] Panigrahi, B. K., Bhuyan, A., Shukla, J., Ray, P. K., & Pati, S. (2021). A comprehensive review on intelligent islanding detection techniques for renewable energy integrated power system. *International Journal of Energy Research*, 45(10), 14085-14116.
- [6] Kumbhar, A., Dhawale, P. G., Kumbhar, S., Patil, U., & Magdum, P. (2021). A comprehensive review: Machine learning and its application in integrated power system. *Energy Reports*, 7, 5467-5474.
- [7] Panda, S., Mishra, D. P., & Dash, S. N. (2018, July). Comparison of ANFIS and ANN techniques in fault classification and location in long transmission lines. In *2018 International Conference on Recent Innovations in Electrical, Electronics & Communication Engineering (ICRIEECE)* (pp. 1112-1117). IEEE.
- [8] Venkata, P., Pandya, V., Vala, K., & Sant, A. V. (2022). Support vector machine for fast fault detection and classification in modern power systems using quarter cycle data. *Energy Reports*, 8, 92-98.
- [9] Samantaray, S. R., Dash, P. K., & Panda, G. (2006). Fault classification and location using HS-transform and radial basis function neural network. *Electric Power Systems Research*, 76(9-10), 897-905.
- [10] Parija, B., Pattanayak, R., & Tripathy, S. K. (2018, August). Faults classification In A Microgrid Using Decision Tree Technique And Support Vector Machine. In *2018 Second International Conference on Green Computing and Internet of Things (ICGCIoT)* (pp. 145-148). IEEE.
- [11] Youssef, O. A. (2009, March). An optimised fault classification technique based on Support-Vector-Machines. In *2009 IEEE/PES Power Systems Conference and Exposition* (pp. 1-8). IEEE.